remote sensing

Article

A New Type of 5G-Oriented Integrated BDS/SON High-Precision Positioning

Wenhua Tong [1,2,3,*], Decai Zou [1,2,3], Tao Han [4], Xiaozhen Zhang [1,2,3], Pengli Shen [1,2,3], Xiaochun Lu [1,2,3], Pengbo Wang [1,2,3] and Ting Yin [1,2,3]

1 National Time Service Center, Chinese Academy of Sciences, Xi'an 710600, China; zdc@ntsc.ac.cn (D.Z.); zhangxiaozhen@ntsc.ac.cn (X.Z.); shenpengli@ntsc.ac.cn (P.S.); luxc@ntsc.ac.cn (X.L.); wangpengbo@ntsc.ac.cn (P.W.); yinting@ntsc.ac.cn (T.Y.)
2 Key Laboratory of Precision Navigation and Timing Technology, Chinese Academy of Sciences, Xi'an 710600, China
3 University of Chinese Academy of Sciences, Beijing 100049, China
4 College of Science, Xi'an University of Technology, Xi'an 713300, China; hantao@xaut.edu.cn
* Correspondence: tongwenhua@ntsc.ac.cn; Tel.: +86-181-1715-9232

Abstract: China is promoting the construction of an integrated positioning, navigation, and timing (PNT) systems with the BeiDou Navigation Satellite System (BDS) as its core. To expand the positioning coverage area and improve the positioning performance by taking advantage of device-to-device (D2D) and self-organizing network (SON) technology, a BDS/SON integrated positioning system is proposed for the fifth-generation (5G) networking environment. This system relies on a combination of time-of-arrival (TOA) and BeiDou pseudo-range measurements to effectively supplement BeiDou signal blind spots, expand the positioning coverage area, and realize higher precision in continuous navigation and positioning. By establishing the system state model, and addressing the single-system positioning divergence and insufficient accuracy, a robust adaptive fading filtering (RAF) algorithm based on the prediction residual is proposed to suppress gross errors and filtering divergence in order to improve the stability and accuracy of the positioning results. Subsequently, a federated Kalman filtering (FKF) algorithm operating in fusion-feedback mode is developed to centrally process the positioning information of the combined system. Considering that the prediction error can reflect the magnitude of the model error, an adaptive information distribution coefficient is introduced to further improve the filtering performance. Actual measurement and significance test results show that by integrating BDS and SON positioning data, the proposed algorithm realizes robust, reliable, and continuous high precision location services with anti-interference capabilities and good universality. It is applicable in scenarios involving unmanned aerial vehicles (UAVs), autonomous driving, military, public safety and other contexts and can even realize indoor positioning and other regional positioning tasks.

Keywords: Beidou Navigation Satellite System; self-organizing network; robust filtering; fading filtering; federated kalman filtering

check for updates

Citation: Tong, W.; Zou, D.; Han, T.; Zhang, X.; Shen, P.; Lu, X.; Wang, P.; Yin, T. A New Type of 5G-Oriented Integrated BDS/SON High-Precision Positioning. *Remote Sens.* **2021**, *13*, 4261. https://doi.org/10.3390/rs13214261

Academic Editor: Stefania Bonafoni

Received: 7 August 2021
Accepted: 20 October 2021
Published: 23 October 2021

1. Introduction

Global navigation satellite system (GNSS), as an indispensable foundation for the collection and management of information on a national scale, has played important roles in traffic management, emergency response, and marine and national defense. With the construction and implementation of the Global Positioning System (GPS) in the United States [1,2], the Global National Satellite System (GLONASS) in Russia [3,4], Galileo in the European Union [5], the BDS in China [6], the Quasi-Zenith Satellite System (QZSS) in Japan, and the Indian Regional Navigation Satellite System (IRNSS) [7], compatibility and interoperability have become major trends in the future development of GNSS, and academic journals and conferences worldwide have published many articles addressing theoretical analyses of compatibility and interoperability [8–10]. In addition, with a focus on the differences between systems [11], time interoperability [12], spatial coordinate interoperability, and positioning and integrity algorithms [13], much research has been performed to date. As an outcome of this research, it has been noted that after the collection, screening and fusion of multi-constellation and multifrequency GNSS data, the dependence on any single constellation is weakened, and the risk of performance degradation or service interruption caused by electromagnetic interference, terrain occlusion, ionospheric scintillation, denial of service or other factors are reduced, significantly improving various navigation performance indicators [14].

However, the GNSS has natural vulnerabilities. The reception power of a satellite signal is only approximately −160 dBW, resulting in poor penetration, and the frequency and structure of such civil signals are open, leaving them vulnerable to deception and interference. Consequently, in cities, forests, complex sheltered areas or complex electromagnetic countermeasure environments, the availability, continuity, robustness and reliability of PNT services cannot be guaranteed. With the gradual expansion of GNSS applications and increasing user demand, related vulnerabilities have gradually been revealed in the context of automatic driving and military and national defense. Therefore, in 2016, China began to promote the construction of an integrated PNT system with BDS as its core [15,16], aiming to achieve high integration of multiple PNT sources and multisource data fusion in order to generate PNT service information as a unified spatial-temporal benchmark with anti-interference and anti-deception capabilities and features of high robustness, availability, continuity, and reliability.

Following this trend, many works have emerged on research and development toward comprehensive service systems. For example, in [13], the differentiation factors and influences between systems, time interoperability, coordinate interoperability and core positioning algorithms are comprehensively and systematically investigated to promote research on GNSS interoperability technology. Ref. [17] summarizes the worldwide development status of low earth orbit (LEO) navigation enhancement constellations, which possess high signal strength, strong anti-interference capabilities and adaptability to fast geometric changes on the ground. Accordingly, LEO constellation can complement medium- and high-orbit GNSS constellations to significantly enhance the positioning accuracy, integrity, continuity, and availability of GNSS. However, due to the low satellite orbits and small single-satellite ground coverage, a multibeam antenna is required to ensure the signal gain in the coverage area, which increases the burden of signal acquisition on the receiver and reduces the signal acquisition speed. In addition, the air resistance in low orbit is high, and the satellite speed and orbit height will gradually decrease, necessitating frequent startup to maintain such an orbit. Hence, due to their limited capacity for carrying fuel resources, these satellites have a short service life. In [18], the unavoidable inherent shortcomings of purely visual navigation algorithms were clarified; specifically, they depend on the texture characteristics of the scene, are easily affected by lighting conditions, and have difficulty dealing with fast rotating motion. Therefore, to improve the stability of a navigation system, the introduction of inertial information was considered, and research progress on the integration of inertial navigation systems (INSs) with visual integrated navigation technology was comprehensively summarized.

In a combined GNSS and radio communication system, the high-precision integration of 5G and BDS can further promote the precise coordination of object in space. For example, [19] studied the integration of the characteristics of the 5G network base station and the GNSS-based enhancement system, to exploit the advantages of 5G network in terming of positioning coverage and data broadcasting in order to expand the scope of GNSS positioning services; to this end, the integration of 5G terminals and high-precision terminals was realized, and the prospects of integrating of 5G and GNSS high-precision positioning were analyzed. In [20], the positioning performance of an integrated system combining 5G base stations and GNSS technology under multipath interference was studied in detail. However, with the explosive growth in the number of terminal devices currently being encountered in many applications, especially in the contexts of UAVs, the Internet of Things and the Internet of Vehicles, the centralized aggregation of terminal signals to a base station for forwarding greatly increases the occupancy rate of frequency band resources and, thus, increases the network load. Therefore, we consider using device-to-device (D2D) communication technology, one of the key technologies of 5G network, to indirectly realize the high-precision integration of 5G and BDS. The most obvious advantage of D2D technology is that users can build a self-organizing network (SON), play the roles of server and client simultaneously, and directly connect to the network without forwarding through a base station, thereby avoiding occupying frequency band resources reserved for cellular wireless communication. Thus, they can realize self-coordination, self-configuration, and self-optimization, reduce the network load and improve the operation efficiency.

Relying on D2D-SON technology, this paper proposes an integrated BDS/SON navigation and positioning system for 5G based on onboard sensors. The SON information is used to enhance and supplement the BDS location service which can not only effectively expand the positioning coverage area and improve the positioning accuracy of BDS but also effectively supplement the blind spots of the BeiDou signal to enable continuous navigation and positioning with the help of the SON system even when the signal is blocked or disturbed. This real-time and higher precision integrated positioning technology can also be extended to multi-frequency and multi-constellation GNSS and applied to many fields, such as autonomous driving, military, and public safety. This is a new application of sensors cooperative work in the field of navigation and positioning.

This paper aims to propose an effective filter estimation technique to improve the performance of carrier navigation and positioning. The traditional Kalman filtering (KF) algorithm offers high real-time performance and high estimation accuracy based on a small amount of data but is suitable only for linear scenarios. Extended Kalman filtering (EKF) is the most common non-linear filtering method and has a very fast calculation speed. It is of great application significance in the fields of target tracking and real-time state estimation. Unscented Kalman filtering (UKF) is suitable only for low-dimensional non-linear state problems. Particle filtering (PF) offers high accuracy and is suitable for use in environments affected by non-Gaussian noise, but as the number of particles increases, the filtering complexity also increases, and the filtering speed decreases significantly [21].

Therefore, for the static positioning scenario to be addressed by the proposed integrated BDS/SON system, this paper starts from the common EKF algorithm and, to overcome the observation anomaly problem for a single system, first proposes a robust adaptive fading filtering (RAF) algorithm to perform local optimal estimation for the BDS and SON subsystems to suppress gross errors and filtering divergence. Furthermore, an improved federated filtering algorithm is constructed to account for the limited application scope and insufficient performance of BDS alone, an adaptive information allocation strategy is implemented, and the positioning results of the SON subsystem are integrated to improve the service performance. Finally, the positioning accuracies of the RAF and federated filtering algorithms are verified and compared, and the effectiveness of the algorithms is analyzed from the perspective of a significance test.

2. Materials and Methods

2.1. Integrated BeiDou Navigation Satellite System (BDS)/Self-Organizing Network (SON) Positioning Model

The application scenario for the proposed integrated positioning system is illustrated in Figure 1. Limited by the signal strength, there is only short-range communication between the SON nodes. The terminal to be tested simultaneously receives multiple BDS satellite signals and ranging signals from multiple SON terminals.

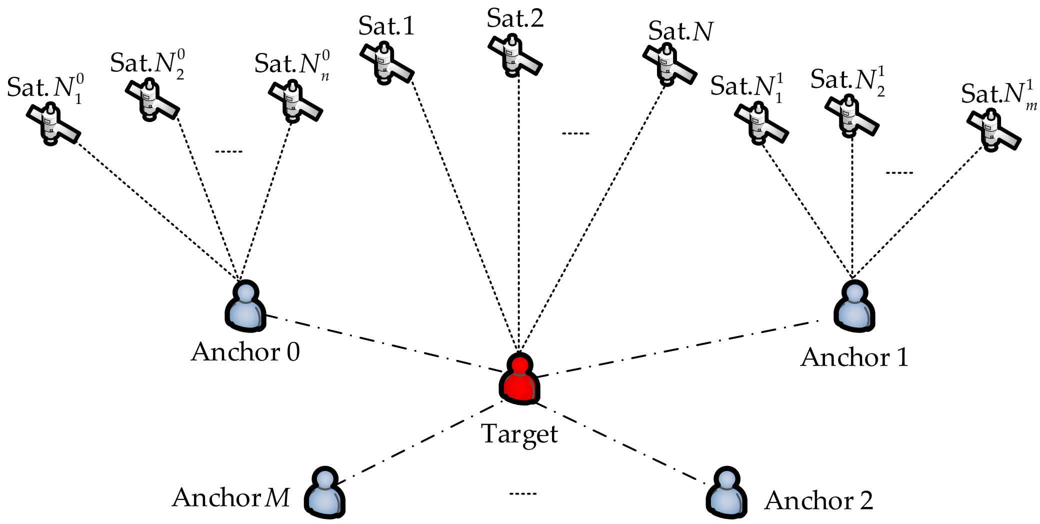

Figure 1. Integrated positioning model.

Now, it is assumed that the node (x_0, y_0, z_0) to be measured can receive $N(N \geq 4)$ BeiDou satellite signals, where the satellite coordinates are $(X_1, Y_1, Z_1), (X_2, Y_2, Z_2), \cdots, (X_N, Y_N, Z_N)$. This node can also form a SON network with its surrounding anchor nodes for information transmission to obtain the ranging values and the location information of these other nodes. Each anchor node has realized separate BeiDou positioning separately, with coordinates $(x_1, y_1, z_1), (x_2, y_2, z_2), \cdots, (x_M, y_M, z_M)$.

2.2. *Robust Adaptive Fading Filtering (RAF) Algorithm*

2.2.1. Kalman Filtering (KF)

KF was first proposed by the American scholar R.E. Kalman in 1960 [22]. The algorithm is recursive. The filter is designed in the time domain using the state space method. It is an optimal autoregressive data processing method that is suitable for state estimation for multidimensional random processes in linear systems. It has two variants: continuous and discrete. In discrete KF, data are detected from the input signal, and a linear equation is used to observe the system state. The system state can be estimated in recursive form from data that contain various types of noise, and by updating and processing the collected data in a timely manner, the amount of data that must be stored for in the estimation process can be kept small, which is beneficial for rapid data processing and suitable for real-time positioning. Hence, this algorithm has been widely used in engineering.

The discretized equations of state and observation equations of the system are as follows [22,23]:

$$x_k = \Phi_{k|k-1} x_{k-1} + w_{k-1} \tag{1}$$

$$z_k = H_k x_k + v_k \tag{2}$$

where x_k is the n-dimensional state vector in time step k, that is, the predicted values for coordinate correction; $\Phi_{k|k-1}$ is the $n \times n$-dimensional state transition matrix; z_k is the m-dimensional observation vector at time k; and H_k is the $m \times n$-dimensional observation matrix. The state noise w_k and the observation noise v_k are uncorrelated zero mean white noise sequences that exhibit the following characteristics [23]:

$$\begin{cases} E(w_k) = 0 \quad Cov\left(w_k w_j^T\right) = Q_k \delta_{k,j} \\ E(v_k) = 0 \quad Cov\left(v_k v_j^T\right) = R_k \delta_{k,j} \\ Cov(w_k, v_j) = 0 \end{cases} \tag{3}$$

$$\delta_{k,j} = \begin{cases} 1, & k = j \\ 0, & k \neq j \end{cases} \tag{4}$$

The conventional KF algorithm can be applied to solve linear problems with Gaussian noise, while the EKF algorithm is more commonly used for handling non-linear systems. Similar to KF, EKF also consists of two recursive update processes. However, in the EKF algorithm, the non-linearity of the problem needs to approximately described by means of local linearization methods such as Taylor series expansion, leading to an observation matrix of the form $H_k = \frac{\partial H(x_k)}{\partial x_k}\Big|_{x_k=\hat{x}_{k|k-1}}$.

The overall filtering process is described as follows:

Time update:

$$\hat{x}_{k|k-1} = \Phi_{k|k-1}\hat{x}_{k-1} \tag{5}$$

$$P_{k|k-1} = \Phi_{k|k-1}P_{k-1}{\Phi_{k|k-1}}^T + Q_{k-1} \tag{6}$$

Observation update:

$$K_{k=}P_{k|k-1}{H_k}^T\left[H_kP_{k|k-1}{H_k}^T + R_k\right]^{-1} \tag{7}$$

$$\hat{x}_k = \hat{x}_{k|k-1} + K_k\left(z_k - H_k\hat{x}_{k|k-1}\right) \tag{8}$$

$$P_k = (I - K_kH_k)P_{k|k-1}(I - K_kH_k)^T + K_kR_k{K_k}^T \tag{9}$$

2.2.2. Adaptive Fading Filtering

Accurate statistical error characteristics and filtering models are the basis for the optimal estimation of the KF/EKF algorithm. Despite the simplicity of the EKF algorithm, the interference caused by external factors in the motion process is usually unknown and unpredictable, and model simplification, inaccurate modeling of the initial system state, and real-time variations in the parameter noise can introduce strong uncertainty into the filter model. In addition, historical data accumulate over time, which restricting the filter estimate at the current moment and affecting the estimation accuracy. At the same time, the KF/EKF algorithm cannot adjust the gain matrix online in response to the real-time state because of the offline nature of its calculations, so it lacks the ability to track state mutations in a challenging environment. As the measurement error increases, the filtering accuracy decreases and may even diverge, leading to poor reliability and robustness.

To solve the above problems, Fagin [24] and Sorenson [25] proposed a filtering algorithm using a fading factor to limit the filter memory length, but they did not consider the optimality of the filter. Xia Qijun [26] proposed a new fading filtering algorithm for linear systems, and Zhou Donghua [27] proposed a strong tracking filtering algorithm based on the EKF algorithm and extended it to non-linear systems. As introduced in Formula (10), a time-varying fading factor was introduced to adjust the prediction covariance matrix in real time to improve the utilization of new data and enhance the filter performance [27]:

$$P_{k|k-1} = \lambda_k\Phi_{k|k-1}P_{k-1}{\Phi_{k|k-1}}^T + Q_{k-1} \tag{10}$$

where, $\lambda_k \geq 1$ is the time-varying fading factor.

According to Formula (8), the predicted residual at a particular point in the KF or EKF algorithm, that is, the innovation sequence, is

$$\varepsilon_k = z_k - H_k\hat{x}_{k|k-1} = z_k - H_k\Phi_{k|k-1}\hat{x}_{k-1} \tag{11}$$

A strong tracking filter keeps track of the actual state of the system by forcing the innovation sequences at different times to remain orthogonal to each other. However, whether the filter is in a stable state is judged based on whether the fading factor calculated in accordance with the innovation covariance is greater than 1, which may lead to the introduction of a fading factor when it is not necessary. Therefore, a new adaptive fading factor is proposed based on filter convergence.

If the filtering model is constructed accurately and the system noise and observation noise are white noise and uncorrelated, the innovation follows a normal distribution with a mean value of 0 and the covariance is

$$E\left(\varepsilon_k {\varepsilon_k}^T\right) = H_k P_{k|k-1} {H_k}^T + R_k = H_k \Phi_{k|k-1} P_{k-1} {\Phi_{k|k-1}}^T {H_k}^T + H_k Q_{k-1} {H_k}^T + R_k \quad (12)$$

when the filtering model diverges, the actual value of the innovation covariance is much greater than the theoretical value; hence, Formula (13) can be used to evaluate the convergence of the filter:

$${\varepsilon_k}^T \varepsilon_k \leq \gamma trace\left[E\left(\varepsilon_k {\varepsilon_k}^T\right)\right] \quad (13)$$

where γ is a reserve coefficient greater than 1. When the above formula is satisfied, the filter is working normally; otherwise, the filter has diverged. When the reserve coefficient is set in advance, the ratio of the variance of the innovation sequence to the trace of theoretical covariance is assumed as follows:

$$a_k = \frac{{\varepsilon_k}^T \varepsilon_k}{trace\left(H_k \Phi_{k|k-1} P_{k-1} {\Phi_{k|k-1}}^T + H_k Q_{k-1} {H_k}^T + R_k\right)} \quad (14)$$

$$a_k = \begin{cases} \gamma, & a_k \geq \gamma \\ a_k, & a_k < \gamma \end{cases} \quad (15)$$

The constructed fading factor is [28],

$$\lambda_k = \begin{cases} e^{a_k - 1}, & a_k \geq 1 \\ 1, & a_k < 1 \end{cases} \quad (16)$$

2.2.3. Robust Filtering

Although adaptive filtering is widely used to modify the state of a filter by introducing the fading factor on the basis of the EKF algorithm to ensure that the state estimate conforms to the convergence condition and improve the system robustness, the gross observation error cannot be eliminated. In some practical application scenarios, the resulting filtering effect is not ideal. In this paper, we classify the gross error into stochastic models using the principle of robust estimation to make the filtering results resistant to the influence of the gross observation error. Let the variance of the observation value z_i be denoted by R_{ii}; then, the equivalent variance can be expressed as $\overline{R}_{ii} = \frac{1}{\omega_i} R_{ii}$, with the equivalent measurement noise covariance matrix $\overline{R}_k$ instead of R_k and a real-time-adjusted filtering gain matrix to realize robust performance [29].

To construct the robust factor, we select the Institute of Geodesy and Geophysics (IGG) three-segment function model [30]:

$$\omega_i = \begin{cases} 1, & |\overline{\varepsilon}_i| \leq c_0 \\ \frac{c_0}{|\overline{\varepsilon}_i|}\left(\frac{c_1 - |\overline{\varepsilon}_i|}{c_1 - c_0}\right), & c_0 < |\overline{\varepsilon}_i| \leq c_1 \\ 0, & |\overline{\varepsilon}_i| > c_1 \end{cases} \quad (17)$$

where c_0 and c_1 are set to 1.5 and 3.0, respectively, and $|\overline{\varepsilon}_i|$ is the standardized residue. The corresponding filtering gain formula, as given in (7), can be rewritten as follows:

$$K_k = P_{k|k-1} {H_k}^T \left[H_k P_{k|k-1} {H_k}^T + \overline{R}_k\right]^{-1} \quad (18)$$

2.3. Integrated Positioning Model and Adaptive Federated Filtering

2.3.1. Federated Filtering Model

In navigation systems that rely on multisource information fusion, federated filters are widely used due to their low computational cost, high precision, and strong fault tolerance and reliability. The central idea is to perform decentralized processing before global fusion, and the main filter possesses strong fault detection, isolation and recovery capabilities for the subfilters.

In this paper, the BDS and SON positioning systems are regarded as two subfilters. As in the RAF model above, the one-step predicted values are modified by using the information of the measured values to obtain the local optimal estimates $\hat{x}_{k,BDS}$ and $\hat{x}_{k,SON}$. The federated Kalman filtering structure of the fusion-feedback mode is selected, the local optimal estimate for each subfilter is input into the main filter for information fusion in accordance with Equations (19) and (20), and finally, the state estimate and the optimal solution for the covariance matrix are output [31].

$$\hat{x}_{k,m} = P_{k,m}\left(P_{k,BDS}{}^{-1}\hat{x}_{k,BDS} + P_{k,SON}{}^{-1}\hat{x}_{k,SON}\right) \tag{19}$$

$$P_{k,m}{}^{-1} = P_{k,BDS}{}^{-1} + P_{k,SON}{}^{-1} \tag{20}$$

The federated filter is adjusted by means of information distribution coefficients [31]:

$$\begin{cases} P_{k,i} = \beta_i^{-1}P_{k,m} \\ Q_{k,i} = \beta_i^{-1}Q_{k,m} \\ x_{k,i} = x_{k,m} \end{cases} \tag{21}$$

where the distribution coefficients $\beta_i > 0$ satisfy the information conservation principle $\beta_{BDS} + \beta_{SON} = 1$.

2.3.2. Information Distribution

As seen from the above discussion, the main filter controls and adjusts the subfilters by means of distribution coefficients, as shown in Formula (21): $\beta_{BDS} = P_{k,m}P_{k,BDS}{}^{-1}$ and $\beta_{SON} = P_{k,m}\,P_{k,SON}{}^{-1}$. The information distribution coefficients control the weighting of the local filters in the main filter. The determination of the coefficients, therefore, directly determines the structure and performance of the filter.

The most intuitive method is to specify fixed distribution coefficients before filtering on the basis of prior information; however, in an integrated navigation system relying on multisource information, the observation quality and performance of each subsystem will vary with time. For example, for the integrated system considered in this paper, the observation quality of the BDS is good in open and unobstructed environments but poor in complex spatial environments due to the occlusion and interruption of the satellite signals. For the SON system, the availability of line-of-sight (LOS) signals based on distance measurements is based on the premise that there are no obstacles between nodes; hence, this system is vulnerable to multipath fading, shadowing effects and multiple access interference, which make the observation quality uncertain. Therefore, it is necessary to adaptively determine the information distribution coefficients by taking into account the influence of the subsystem models and observation quality [32].

In estimation theory, the prediction residual reflects the magnitude of the model error for most the kinematic models. Therefore, this paper presents an adaptive factor solution based on the prediction residual. According to the distribution characteristics of the residuals in Formula (13), statistics are constructed as follows.

$$b_{i,k} = \frac{\varepsilon_k{}^T\varepsilon_k}{trace\left(H_kP_{k|k-1}H_k{}^T + \overline{R}_k\right)} \tag{22}$$

Because robust filtering is used in the subfilters, only a two-segment structure is used to estimate the adaptive information distribution coefficients. When the statistics satisfy $|b_{i,k}| \leq c$, the system state model is considered to be accurate, meaning that the observation information is effective, and the performance of the local filter is good; otherwise, observation anomalies may occur.

$$\beta'_{i,k} = \begin{cases} 1, & |b_{i,k}| \leq c \\ \frac{c}{|b_{i,k}|}, & |b_{i,k}| > c \end{cases} \tag{23}$$

where c is an empirical constant with a value in the range of 0.85 to 1. Finally, the adaptive distribution coefficients should be normalized to satisfy the information conservation principle.

This section has discussed the principle of the adaptive federated filtering algorithm, which uses a robust adaptive filtering algorithm in the subfilters to improve positioning accuracy and to suppress gross errors and filtering divergence. In the main filter, the coefficients are assigned in accordance with the a posterio residuals, and the global estimation results are fed back to the subfilters to ensure the filtering performance.

3. Results

To verify the performance of the federated filtering algorithm in the proposed integrated system based on RAF in each subsystem, a set of BDS/SON data collected on the football field at the Xi'an National Time Service Center, Chinese Academy of Sciences, was used for testing. The BDS-related data were collected using from a multisystem multi-frequency high-precision GNSS receiver with UR4B0-D model, and six SON positioning terminals were used to collect the precise real-time kinematic (RTK) coordinates of five anchor nodes and the distance between each anchor node and an unknown node; then, all observation information was transmitted to the unknown node for the positioning calculation. The sampling rate and sampling time were 1 Hz and 1000 epochs, respectively, and all SON terminals have realized time synchronization characteristics. In this paper, the positioning solution is expressed in the BeiDou coordinate system (BDCS) [33]. By introducing the RTK technology, the mean value of the positioning result with centimeter accuracy obtained by the SON equipment of the node to be tested within the sampling time on one day, is taken as the true value for reference. The final positioning error results are presented and compared in an ENU coordinate system with the true reference RTK coordinates as the origin. The data processing model and the parameters of the system are shown in Table 1.

Table 1. Model and parameter settings for data processing.

Parameter	Model
Device of unknown node	GNSS receiver and SON terminal
Equipment of anchor node	SON terminal
Observations	Pseudo and range observations
Sampling rate	1 Hz
Satellite system	BDS
Coordinate system	BDCS
Signal	BDS B1I + BDS B3I + SON
Satellite ephemerides	Broadcast ephemeris
Cutoff elevation	15 degrees
Ionospheric delay correction	Ionosphere-free combination
Ionospheric delay correction	Dual frequency correction
SON clock difference	Time synchronization
Station displacement	Fixed; estimated for static positioning
True station coordinates	B = 34.3691911165060 L = 109.2222237032327 H = 477.0780838084403 m

3.1. BDS and SON Single-System Tests

Positioning was performed for the individual BDS and SON systems using the weighted least squares (WLS) algorithm, the EKF algorithm and the RAF algorithm proposed in this paper, and the processed results were compared with the true values for reference. The pseudo-range observation noise of the initial BDS was set to 5 m and the distance observation noise of the SON system was set to 1 m.

The comparison and verification of the three solution methods were carried out for each of the three directions: east, north, and up. The positioning error results are shown in Figures 2 and 3, where the WLS method is based on the height angle and the measurement distance in the BDS and SON systems. Tables 2 and 3 present comparisons of the errors of the different positioning algorithms in the BDS and SON systems, respectively.

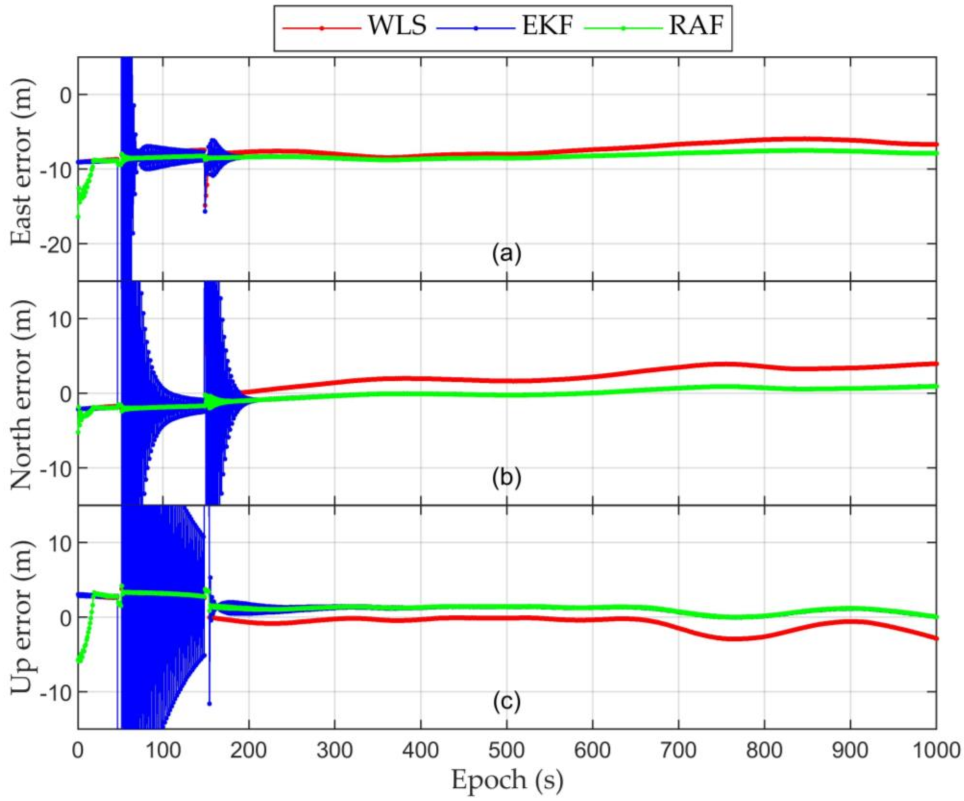

Figure 2. Positioning errors of the BDS with different calculation methods: (**a**) East component; (**b**) North component; (**c**) Up component.

Table 2. Statistical results for the mean and root mean square positioning errors of the BDS under different solution strategies.

Algorithm		Mean Value (m)			RMSE (m)		
		E	N	U	E	N	U
BDS_WLS		−11.03	4.35	−5.92	63.65	41.20	136.77
BDS_EKF		−10.05	1.12	−1.50	44.23	27.01	72.21
BDS_RAF		−8.30	−0.21	1.13	8.33	0.96	1.63
Improvement	RAF-WLS		—		86.91%	97.67%	98.81%
	RAF-EKF				81.17%	96.45%	97.74%

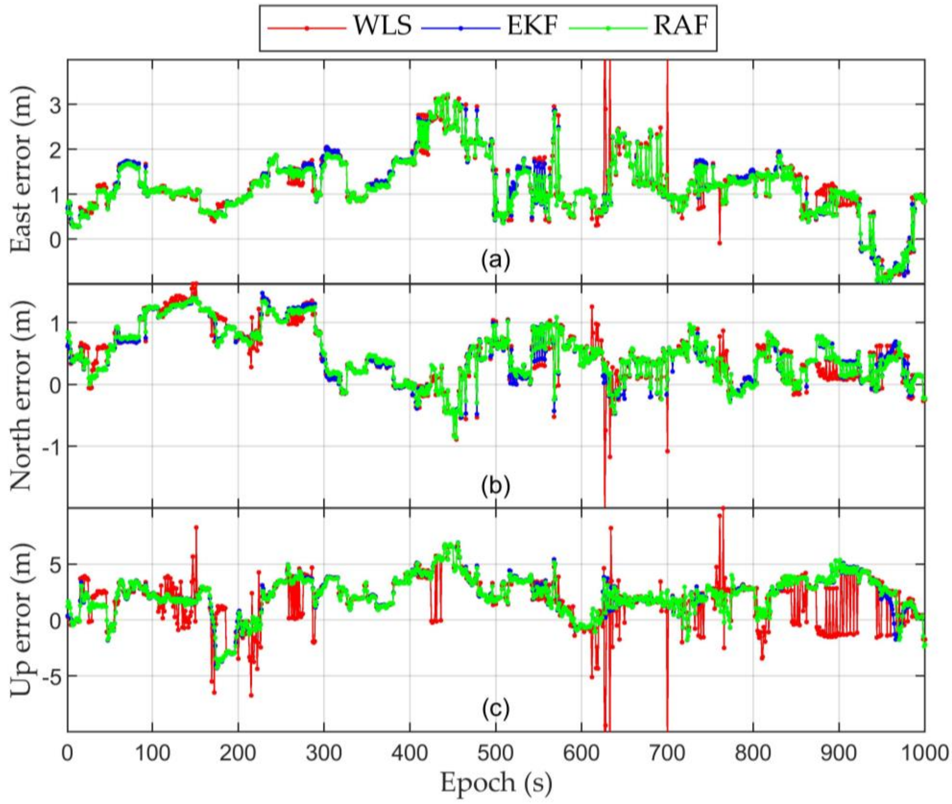

Figure 3. Positioning errors of the SON system with different calculation methods: (**a**) East component; (**b**) North component; (**c**) Up component.

Table 3. Statistical results for the mean and root mean square positioning errors of the SON system under different solution strategies.

Algorithm		**Mean Value (m)**			**RMSE (m)**		
		E	**N**	**U**	**E**	**N**	**U**
SON_WLS		1.20	0.47	1.81	1.41	0.66	2.91
SON_EKF		1.18	0.47	2.16	1.38	0.65	2.80
SON_RAF		1.16	0.48	2.17	1.36	0.65	2.79
Improvement	RAF-WLS		—		3.55%	1.52%	4.12%
	RAF-EKF				1.45%	0	0.36%

For the BDS individually, according to Figure 2 and Table 2, the WLS algorithm can obtain effective positioning results; however there is no correlation between the solutions for previous and subsequent epoch, the amount of calculation is large, and the uncertainty of the observation quality leads to large positioning fluctuations and instability. Due to its iterative characteristics, the amount of computation in the EKF algorithm is much less than that in the WLS algorithm, and its robustness and accuracy after convergence are improved compared with those of the WLS algorithm; however in the first 200 epochs, under the influence of abnormal observations, the positioning results are seriously distorted, and the robustness and availability are poor. Consequently, the EKF algorithm has great limitations in practical application. In contrast, the RAF algorithm inherits the epoch correlation characteristics of the EKF algorithm and requires only a small amount of calculation. At the same time, the introduction of the robust factor and the adaptive fading factor allows the algorithm to effectively resist gross observation errors and suppresses filter divergence, especially in the first 200 epochs. In the east, north, and up components, the root mean square error (RMSE) of the RAF algorithm is improved compared to that of the WLS algorithm by 86.9%, 98.0%, and 98.8%, respectively, while the corresponding improvements compared with the EKF algorithm are 81.2%, 96.4%, and 97.7%, respectively. Hence, the positioning accuracy, effectiveness, and robustness in all three directions are significantly improved.

Similarly, Figure 3 and Table 3 present the positioning error comparison for the individual SON system. Because the original observation signals are a short-range LOS distance signals with few errors and good observation quality, the overall positioning accuracy of the SON system is much higher than that of the BDS. Because of the lack of correlation between epochs, the positioning accuracy of the WLS algorithm shows distinct changes in certain epochs with high or low observation quality. The EKF algorithm uses all the historical data in the solution process to offset the errors caused by epochs with poor observation quality, but this approach also degrades the higher precision performance that could be achieved on the basis of high-quality observations; hence, although its performance is more stable situation than that of the WLS algorithm, and the overall error level is basically the same. Meanwhile, the RAF algorithm exhibits characteristics similar to those of the EKF algorithm, with little variation in performance.

By analyzing and comparing the positioning results of the three positioning methods between the two individual subsystems, we can see that the RAF algorithm proposed in this paper has an inhibitory effect on the influence of gross observation errors, especially for the positioning results of the BDS in the first 200 epochs. Compared with the WLS algorithm, it can improve the positioning accuracy and enhance the reliability and robustness of each single positioning system, especially in harsh environment.

3.2. Test of the Integrated BDS/SON Positioning System

It is clear from the above analysis that the positioning accuracy and robustness of the SON system are better than those of the BDS; however, the range of the SON system is short, and its navigation and positioning performance depends on the accuracy and strength of the internode distance measurements. For nodes in complex and dynamic environments, non-line-of-sight (NLOS) interference and other factors seriously affect the distance observation quality. Moreover, the SON needs to be frequently reconstructed to meet the positioning requirements as the nodes move, increase the positioning complexity while also reducing the positioning reliability and availability. Consequently, the SON system is not suitable to be applied as an independent positioning system. Therefore, we integrate the BDS and SON systems, combine the communication signals and positioning signals, and use the SON system to assist the BDS in realizing continuous navigation and positioning in complex environment, to expand the positioning coverage area and improve the positioning accuracy relative to BDS positioning alone.

Figure 4 shows the positioning results obtained by applying the federated Kalman filter (FKF) algorithm in the dual system based on the two subsystems with RAF to compare and verify the positioning results of the BDS and SON subsystems in the east, north, and up directions. Table 4 shows the positioning error statistics. With the introduction of the adaptive information distribution coefficients, the RMSE of the federated filter in the east and north components are increased by 33.9% and 17.7%, respectively, compared to those of the BDS subsystem, while the RMSE in the up component is decreased relative to that of the BDS subsystem but is increased by 17.6% compared to that of the SON subsystem. Hence, the positioning accuracy of the dual system lies between those of the two subsystems.

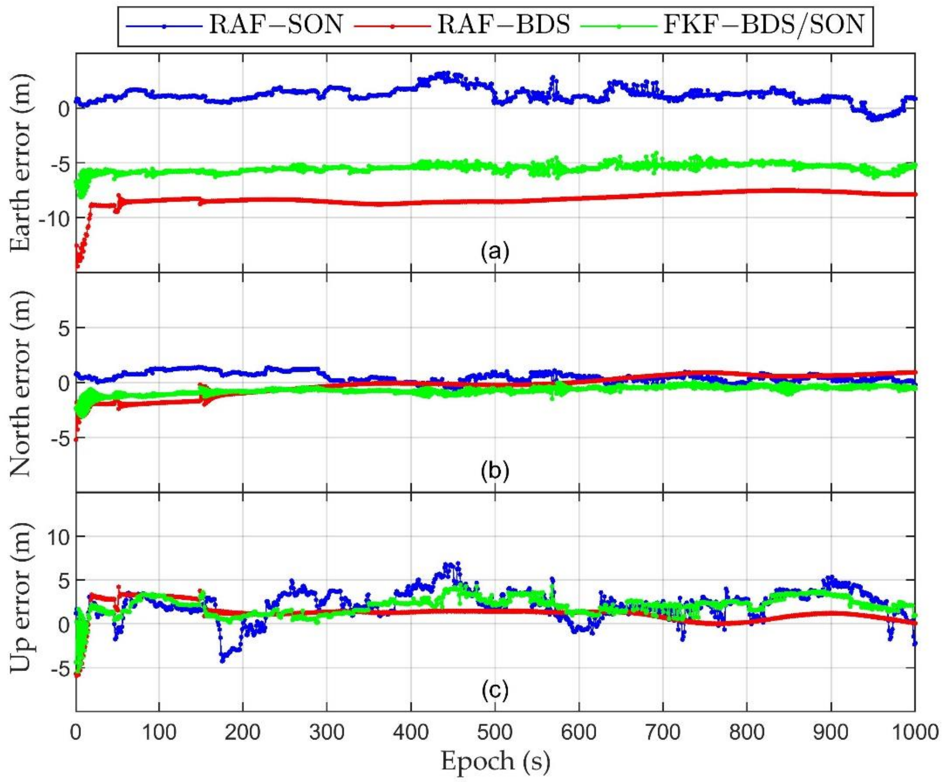

Figure 4. Positioning error of the dual system with federated filtering based on single systems with RAF: (**a**) East component; (**b**) North component; (**c**) Up component.

Table 4. Comparison of the positioning algorithm errors between the dual system with federated filtering and the single systems with RAF.

Algorithm		**Mean Value (m)**			**RMSE (m)**		
		E	**N**	**U**	**E**	**N**	**U**
SON_RAF		1.17	0.48	2.17	1.36	0.65	2.79
BDS_RAF		−8.30	−0.21	1.25	8.33	0.96	1.63
BDS/SON_FKF		−5.49	−0.70	2.05	5.50	0.79	2.30
Improvement	FKF-BDS_RAF		—		33.97%	17.71%	—
	FKF-SON_RAF				—	—	17.56%

Figure 5 shows the positioning error trajectories of the individual BDS system with the RAF algorithm (in red) and dual system with the federated filter (in blue), as well as their projections all in three planes. The BDS alone always shows a large deviation in the east direction, about 7–8 m, which is caused by the poor observation quality due to the interference from trees, tall buildings and many antennas in the east-west direction at the experimental site; however, the positioning accuracy of the BDS in the east direction can be significantly improved after the integration of the SON system. Based on the further analysis in Table 4, the RMSE in the north component is smallest in the SON system, intermediate in the dual BDS/SON system and largest in the BDS, therefore, the integrated system also effectively improves the positioning accuracy of the individual BDS in the north direction. In contrast, the RMSE in the up component is smallest in the BDS, followed by the dual BDS/SON system, and the up-direction RMSE of the SON system is the largest. This is due to the constraints of the experiment, in which the nodes of the SON system all lay in the approximately same horizontal plane, with only small height differences; consequently, the ranging error between nodes had a greater impact on the up component, and at the same time, the positioning error of each anchor node in the up direction was superimposed. Thus, the positioning results for the measured node fluctuated greatly in this direction. As a result, after the integration of the two systems, the overall positioning results show fluctuations in the up component that are larger than those of the BDS alone, and the positioning accuracy is slightly reduced.

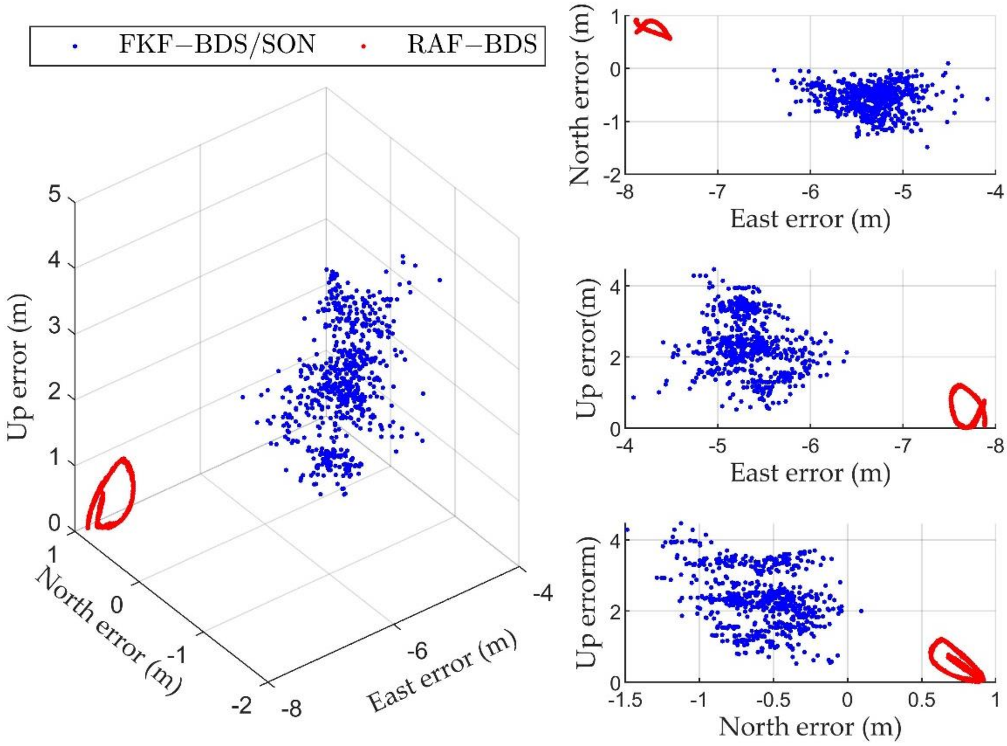

Figure 5. Positioning trajectories and projections under the BDS and integrated systems.

From the above results, it can be seen that joint positioning based on the proposed dual system can balance the error impacts of the errors of two individual subsystems, effectively suppressing the errors caused by a single inaccurate model and resulting in good robustness and reliability.

4. Discussion

To reduce the influence of the randomness of the experimental samples and further analyze the positioning effectiveness of the FKF algorithm in the proposed dual system compared with that of the RAF algorithm in the BDS alone, the significance test method is adopted. At a significance level of $\alpha = 0.05$, three test models are established based on the mean and variance of the positioning errors, as illustrated in the following, taking the variance as an example: (1) two-sided test: the null hypothesis is $H_0 : {\sigma_1}^2 = {\sigma_2}^2$, and the alternative hypothesis is $H_1 : {\sigma_1}^2 \neq {\sigma_2}^2$; (2) Left-sided test: the null hypothesis is $H_0 : {\sigma_1}^2 \geq {\sigma_2}^2$, and the alternative hypothesis is $H_1 : {\sigma_1}^2 < {\sigma_2}^2$; (3) Right-sided test: the null hypothesis is $H_0 : {\sigma_1}^2 \leq {\sigma_2}^2$, and the alternative hypothesis is $H_1 : {\sigma_1}^2 > {\sigma_2}^2$. For the variance, the test statistic $F = S_1^2/S_2^2$ is constructed and judged, where ${\sigma_1}^2$ and ${\sigma_2}^2$ are the variance estimates of the two solution methods and S_1^2 and S_2^2 are the uniformly minimum variance unbiased estimates (UMVUEs). The mean value is determined using the Aspin–Welch test method, and the test statistic for the mean is calculated as $T = \left(\overline{X}_1 - \overline{X}_2\right) / \sqrt{\frac{S_1^2}{n_1} + \frac{S_2^2}{n_2}}$.

Figure 6 shows the significance test results for the differences in the variance and mean, with red asterisks indicating the values of the test statistics, and blue areas indicating the rejections for the hypothesis tests. When the result for a test statistic lies within the rejection, this indicates that the null hypothesis of the test is rejected, that is, its alternative hypothesis is accepted. For the east, north and up components, Figure 6a presents the results of left-, left-, and two-sided tests, respectively, and Figure 6b shows the results of right-, left-, and right-sided tests, respectively. According to the test results in Figure 6 and Table 5, the mean value of the north-component positioning error of the dual system with the FKF algorithm is significantly less than that of the individual BDS, while the mean error values in the east and up components are significantly greater than those of the individual BDS with the RAF algorithm. This is because the error sample data for the east component used in this test have a negative form, and the actual physical significance indicates that the error of the FKF algorithm in the east component is significantly reduced. The significant increase in the up component is due to the influence of the SON system. At the same time, the variances of the positioning errors of the dual system with the FKF algorithm in the east and north components are significantly less than those of the individual BDS with the RAF algorithm, indicating that the error dispersion is reduced and the positioning robustness is further improved; however, the overall difference between the two methods is not statistically significant because the difference in the up component is not significant.

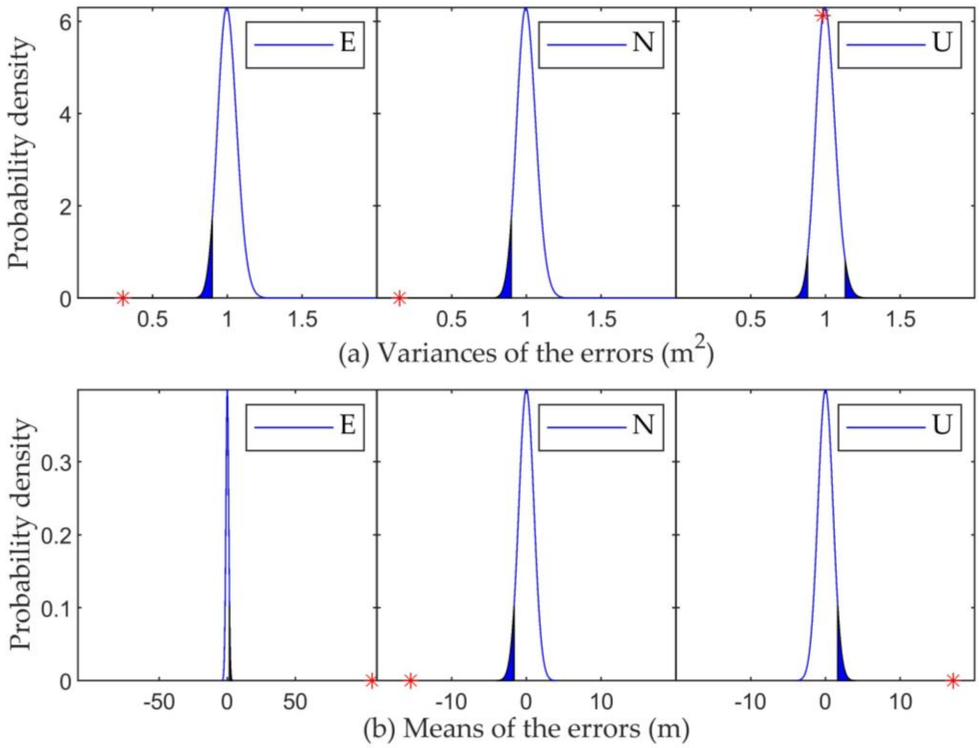

Figure 6. Significance tests of the differences in the means and variances of the errors, with red asterisks indicating the values of the test statistics.

Table 5. Significance test results for the error differences.

Significance Test	Variance			Mean		
	E	N	U	E	N	U
Two-sided	${\sigma_1}^2 \neq {\sigma_2}^2$	${\sigma_1}^2 \neq {\sigma_2}^2$	${\sigma_1}^2 = {\sigma_2}^2$	$\mu_1 \neq \mu_2$	$\mu_1 \neq \mu_2$	$\mu_1 \neq \mu_2$
Left-sided	${\sigma_1}^2 < {\sigma_2}^2$	${\sigma_1}^2 < {\sigma_2}^2$	${\sigma_1}^2 \geq {\sigma_2}^2$	$\mu_1 \geq \mu_2$	$\mu_1 < \mu_2$	$\mu_1 \geq \mu_2$
Right-sided	${\sigma_1}^2 \leq {\sigma_2}^2$	${\sigma_1}^2 \leq {\sigma_2}^2$	${\sigma_1}^2 \leq {\sigma_2}^2$	$\mu_1 > \mu_2$	$\mu_1 \leq \mu_2$	$\mu_1 > \mu_2$

After verification and analysis of this experiment, although the up-component positioning accuracy of the dual system with the FKF algorithm is lower than that of the individual BDS, the influence of the ranging error on the up component could be reduced by increasing the height differences among the nodes in the SON system in practical application, to improve the positioning accuracy. Therefore, it is considered that the dual

BDS/SON system with the FKF algorithm based on individual subsystems with the RAF algorithm proposed in this paper can improve the overall positioning accuracy, suppress gross BDS observation errors and filter divergence, and offer improved positioning system robustness, availability, and reliability.

5. Conclusions

In summary, in a positioning system that relies on BDS signals alone, when abnormal observations occur, the results of the WLS algorithm are relatively stable; however there is no correlation between the previous and subsequent epochs, the amount of calculation is large, and the accuracy is low. Meanwhile, the results of the EKF algorithm fluctuate greatly and continue to affect the positioning results in subsequent epochs, indicating that the influence of gross errors and filter divergence cannot be well controlled. To address these shortcomings, a robust factor and an adaptive fading factor are developed on the basis of the innovation sequence and used to formulate a RAF algorithm that has a good ability to resist gross errors and mitigate divergence. The calculation is simple and takes into account the performance and solution efficiency of the system.

Additionally, the experimental analysis shows that the overall positioning performance of the SON system is better than that of the BDS, however, the SON system is greatly affected by NLOS interference and other factors. Therefore, in complex dynamic scenarios, the nodes to be tested need to frequently reconstruct the SON network, which not only increases the positioning complexity, but also reduces the reliability and availability of positioning. Consequently, as a standalone positioning system, the applicability of the SON system is limited.

Therefore, based on the use of the RAF algorithm in each individual subsystem, we propose a dual BDS/SON system federated that relies on a FKF algorithm, in which adaptive information distribution coefficients are adopted to improve the BDS positioning performance. We evaluate the performance of this integrated system on the basis of error estimation theory, considering significance tests of the differences in the means and variances of the positioning errors. The results indicate that the positioning accuracy and robustness of the dual system with the FKF algorithm in the north and east directions are significantly better than those of the individual BDS with the RAF algorithm. Due to the small height differences among the SON nodes in the experimental environment, the ranging error has a great impact on the up component, which significantly reduces the positioning accuracy of the dual system in this direction, while the difference in robustness is not significant. Combined with the anti-gross error and anti-divergence capabilities of the RAF algorithm for the BDS, overall, it is considered that the dual system with the FKF algorithm proposed in this paper can improve the accuracy, robustness, reliability, and availability of the ordinary BDS.

Therefore, considering that D2D-SON technology is a key technology for 5G communication, we believe that BDS/SON integration is a feasible technical means to achieve the deep integration of 5G and BDS. Taking the BDS information as the core and based on the coordinate datum and time datum corresponding to BDS, the importance of the integrity of a single system will be weakened, and the fault tolerance and error compensation capabilities based on the fusion of multisource information will be improved. In addition, through the auxiliary function of the SON system, it can even supplement the signal blind spots of the BDS in some sheltered areas, and finally support greater region, accuracy, robustness, reliability and availability of location services. This technology can also be extended to multi-frequency and multi-constellation GNSS.

In addition, the influence of atmospheric effect on GNSS signal propagation is the main interference parameter in navigation and positioning applications. Due to different physical characteristics, its research is usually divided into ionosphere and troposphere. Compared with the low temporal and spatial resolution of traditional atmospheric parameter detection methods, parameter retrieval through GNSS observation has obvious advantages. For example, the time resolution of observation is high; It has the characteristics of all-day and all-weather continuous operation, so there has high research value.

Starting from the research results of this paper, with the help of the high-precision time synchronization and positioning characteristics between terminals, it provides a solution for the subsequent distributed multi-station joint retrieval of the parameter characteristics of the atmospheric puncture point above the observation area. Compared with single reference station PPP technology, retrieving atmospheric parameters through distributed multi-station joint GNSS observation can improve the spatial and temporal resolution of observation and realize the monitoring of small- and medium-scale spatial environmental changes. Through appropriate parametric modeling strategies, we can build regional total electron content modeling and accuracy measures and forecast models, tropospheric gradient models, detect the characteristics of atmospheric water vapor change and assimilate it into numerical weather prediction models, and even can provide valuable information on many applications, such as natural disaster detection and climate research. Additionally, accurate tropospheric and ionospheric data can also be fed back to the terminals in the region through the established regional model, which can further enhance GNSS positioning, especially for users with single frequency receivers or areas without ionospheric detection stations, with remarkable effects. This will make a new contribution to the application of remote sensing in geoscience, with abundant sensing data provide good external conditions for the development of this new method and new application.

Author Contributions: Conceptualization, D.Z. and X.L.; methodology, W.T.; software, W.T. and P.S.; validation, W.T. and T.H.; formal analysis, W.T., D.Z. and T.H.; resources, W.T., X.Z. and T.Y.; data curation, W.T. and P.W.; writing—original draft preparation, W.T.; writing—review and editing, D.Z. and T.H.; project administration, D.Z. and X.Z. All authors have read and agreed to the published version of the manuscript.

Funding: This research was funded by the National Natural Science Foundation of China (grant number 41974032), and the Natural Science Foundation of Shanxi province, China (grant number 2021JM-323).

Institutional Review Board Statement: Not applicable.

Informed Consent Statement: Not applicable.

Data Availability Statement: The data that support the findings of this study are available from the corresponding author upon a reasonable request.

Conflicts of Interest: The authors declare no conflict of interest.

References

1. Barnes, D. GPS Status and Modernization. Presentation at Munich Satellite Navigation Summit 2019. Available online: https://apps.dtic.mil/dtic/tr/fulltext/u2/a550403.pdf (accessed on 14 September 2021).
2. Hegarty, C.J. The Global Positioning System (GPS). In *Springer Handbook of Global Navigation Satellite Systems*; Teunissen, P.J., Montenbruck, O., Eds.; Springer: Cham, Germany, 2017; pp. 197–218.
3. Urlichich, Y.; Karutin, S.; Testoedov, N.; Koblov, S. Directions 2021: GLONASS on the Verge of a New Decade. Available online: https://www.gpsworld.com/directions-2021-glonass-on-the-verge-of-a-new-decade/ (accessed on 14 September 2021).
4. Langley, R.B. Innovation: GLONASS—Past, Present and Future. Available online: https://www.gpsworld.com/innovation-glonass-past-present-and-future/ (accessed on 14 September 2021).
5. Benedicto, J.; Costa, R.D. Directions 2021: Galileo Expands and Modernizes Global PNT. Available online: https://www.gpsworld.com/directions-2021-galileo-expands-and-modernizes-global-pnt/ (accessed on 14 September 2021).
6. China Satellite Navigation Office. Development of the BeiDou Navigation Satellite System (Version 4.0). December 2019. Available online: http://m.beidou.gov.cn/xt/gfxz/201912/P020191227430565455478.pdf (accessed on 14 September 2021).
7. Kogure, S.; Ganeshan, A.S.; Montenbruck, O. Regional Systems. In *Springer Handbook of Global Navigation Satellite Systems*; Teunissen, P.J., Montenbruck, O., Eds.; Springer: Cham, Germany, 2017; pp. 305–337.
8. Gibbons, G. GNSS interoperability. *Ins. GNSS* **2011**, *6*, 28–31.
9. Yang, Y.X.; Lu, M.Q.; Han, C.H. Some notes on interoperability of GNSS. *Acta Geod. Cartogr. Sin.* **2016**, *45*, 253–259.
10. Liu, T.X. Interpretation of compatibility and interoperability of satellite navigation systems. *Satell. Netw.* **2017**, 26–37.
11. Zhang, X.Z.; Lu, X.C.; Han, T. Quantitative analysis of improvement of availability and continuity in service performance for users under interoperable GNSS. *J. Time Freq.* **2014**, *37*, 173–180.

12. Wu, H.T. *Time Basis of Satellite Navigation System*; Science Press: Beijing, China, 2011.
13. Han, T. Research on Interoperability Algrithm of Global Navigation Satellite System. Ph.D. Thesis, National Time Service Center, Chinese Academy of Sciences, Xi'an, China, June 2016.
14. Yang, Y.X.; Li, J.L.; Xu, J.Y.; Tang, J.; Guo, H.R.; He, H.B. Contribution of the compass satellite navigation system to global PNT users. *Chin. Sci. Bull.* **2011**, *56*, 1734–1740. [CrossRef]
15. Yang, Y.X. Concepts of comprehensive PNT and related key technologies. *Acta Geod. Cartogr. Sin.* **2016**, *45*, 505–510.
16. Yang, Y.X. Resilient PNT concept frame. *Acta Geod. Cartogr. Sin.* **2019**, *2*, 1–7.
17. Zhang, X.H.; Ma, F.J. Review of the development of LEO navigation-augmented GNSS. *Acta Geod. Cartogr. Sin.* **2019**, *48*, 1073–1087.
18. Zhang, L.L.; Qu, H.; Mao, J.; Hu, X.P. A survey of intelligence science and technology integrated navigation technology. *Navig. Position. Timing* **2020**, *7*, 50–63.
19. Chen, Y.R. The analysis of convergence between 5G and BeiDou high-accuracy positioning. *Telecom Eng. Tech. Stand.* **2020**, *33*, 1–6.
20. Peng, Y.Z.; Tian, Y.; Zhang, W.C.; Peng, A.; Hong, X.M. Positioning accuracy analysis for 5G/GNSS fusion system. *J. Xiamen Univ. (Nat. Sci.)* **2020**, *59*, 101–107.
21. Liu, X.Y. Several typical nonlinear filtering algorithms and performance analysis. *Ship Electron. Eng.* **2019**, *39*, 32–36.
22. Kalman, R.E. A new approach to linear filtering and prediction problems. *J. Basic Eng.* **1960**, *82*, 35–45. [CrossRef]
23. Fu, M.Y.; Deng, Z.H.; Zhang, J.W. *Kalman Filtering Theory and Its Application in Navigation System*; Science Press: Beijing, China, 2003.
24. Fagin, S.L. Recursive linear regression theory, optimal filter theory and error analyses of optimal systems. *IEEE Interat. Conv. Rec.* **1964**, *12*, 216–240.
25. Sorenson, H.W.; Sacks, J.E. Recursive fading memory filtering. *Inf. Sci.* **1971**, *3*, 101–119. [CrossRef]
26. Xia, Q.J.; Sun, Y.X.; Zhou, C.H. An optimal adaptive algorithm for fading kalman filter and its application. *Acta Autom. Sin.* **1990**, *4*, 210–216.
27. Zhou, D.H.; Xi, Y.G.; Zhang, Z.J. Suboptimal fading extented kalman filtering for nonlinear systems. *Control. Decis.* **1990**, *4*, 1–6.
28. Qiu, W.Y.; Li, R.B.; Liu, J.Y. Research on GNSS/MINS integrated navigation algorithm of general aviation based on improved adaptive fading kalman filter. *Electron. Meas. Technol.* **2020**, *43*, 95–100.
29. Miao, Y.W.; Sun, F.P.; Li, F.; Jing, X.P. Research on application of tightly coupled INS/GNSS based on robust extended kalman filter. *J. Geod. Geodyn.* **2013**, *33*, 97–101.
30. Yang, Y.X. *Adaptive Navigation and Kinematic Positioning*; Surveying and Mapping Press: Beijing, China, 2006.
31. Deng, Z.L.; Yin, L.; Yang, L.; Yu, Y.P.; Xi, Y. Location information fusion algorithm for GPS/Base-Station positioning system based on federated kalman filter. *J. Beijing Univ. Posts Telecommun.* **2013**, *36*, 32–36.
32. Duan, R.; Zhang, X.H.; Zhu, F. Adaptive federated filter for multi-sources information fusion in integrated navigation system. *Syst. Eng. Electron.* **2018**, *40*, 267–272.
33. China Satellite Navigation Office. BeiDou Coordinate System. Available online: http://www.beidou.gov.cn/yw/gfgg/201912/W020191209571126683306.pdf (accessed on 14 September 2021).